Dalton Transactions

Accepted Manuscript

ROYAL SOCIETY OF CHEMISTRY

www.rsc.org/dalton

Dalton Transactions

RSCPublishing

ARTICLE

Synthesis and characterization of an immobilizable photochemical molecular device for H_2-generation

Cite this: DOI: 10.1039/x0xx00000x

Received 00th January 2012,
Accepted 00th January 2012

DOI: 10.1039/x0xx00000x

www.rsc.org/

Markus Braumüller[a], Martin Schulz[bc], Dieter Sorsche[a], Michael Pfeffer[a], Markus Schaub[a], Jürgen Popp[c], Byung-Wook Park[d], Anders Hagfeldt[e]*, Benjamin Dietzek[bcf]* and Sven Rau[a]*.

With $[Ru^{II}(bpyMeP)_2tpphzPtCl_2]^{2+}$ **(4)** a molecular photocatalyst has been synthesized for visible-light-driven H_2-evolution. It contains the ligand bpyMeP (4,4'-bis(diethyl-(methylene)-phosphonate)-2,2'-bipyridine) with phosphate ester groups as precursors for the highly potent phosphonate anchoring groups, which can be utilized for immobilization of the catalyst on metal-oxide semiconductor surfaces. The synthesis was optimized with regard to high yields, bpyMeP was fully characterized and a solid-state structure could be obtained. Photophysical studies showed that the photophysical properties and the localization of the excited states are not altered compared to similar Ru-complexes without anchoring group precursors. **(4)** was even more active in homogenous catalysis experiments than $[Ru^{II}(tbbpy)_2tpphzPtCl_2]^{2+}$ **(6)** with tbbpy (4,4'-bis(*t*butyl)-2,2'-bipyridine) as peripheral ligands. After hydrolysis **(4)** was successfully immobilized on NiO, suggesting that an application in photoelectrosynthesis cells is feasible.

Introduction

The sensitization of semiconductors (SC) to prepare dye sensitized photoelectrosynthesis (DSPECs) or photovoltaic cells (DSSCs) is a research area with growing interest.[1–3] Here immobilization of a suitable chromophore or photocatalyst on these semiconductors is a crucial factor. The photosensitizer should have anchoring groups to strongly bind the dye onto the SC surface and to facilitate the charge carrier injection into the SC.[2] The most studied class of surface binding groups in DSSCs and DSPECs are carboxylates and phosphonates. Both are utilized on n-type SCs like TiO_2 as well as on p-type SCs like NiO. Comparisons of DSSCs based on differently functionalized $[Ru^{II}(bpy)_3]^{2+}$ on nanocrystalline NiO demonstrate that higher solar energy conversion efficiencies are obtained in the following order $-CH_2PO_3H_2$ >-COOH >-catechol >-CSSH.[4] Additionally, methyl phosphonic acid and carboxylic acid display the highest affinity and monolayer coverage for NiO, which can be monitored by resonance Raman microspectroscopy that can also be used to assure the quality of dye sensitized NiO films.[5] Recently it could be shown, that the conjugation of a molecular photocatalyst to a NiO surface did lead to electron transfer from the surface to the catalytic centre which in turn lead to hydrogen formation.[6] Within the context of molecular photocatalysts, tpphz based multinuclear complexes are of great interest as it contains a redoxactive side which can store electrons more efficiently than e.g. bpy ligands (tpphz = tetrapyrido[3,2-a:2',3'c:3'',2'',-h:2''',3'''-j]phenazine, bpy = 2,2'-bipyridine).[7] The H_2-evolving activity of palladium(II)-based Ru^{II}-tpphz-Pd^{II} photocatalysts have been extensively investigated so far in our group.[7–10] However the hydrogen production is accompanied with the formation of colloidal Pd(0), since the stability of the zero valent metal centre is too low in the N^N chelating sphere of tpphz.[11] A related complex $[Ru^{II}(tbbpy)_2tpphzPtCl_2]^{2+}$ has been reported by Eisenberg *et al.* as early as 1998.[12] The possible application of this complex as intramolecular photocatalyst has recently been reported.[11] In contrast to the analogous palladium catalyst high chemical stability under photocatalytic hydrogen evolving conditions was observed. However relatively low catalytic activity (max. turnover number of 7) was reported as well.

Homodinuclear Ru-tpphz complexes have already been bound via carboxylated bipyridine ligands to semiconducting TiO_2 electrodes.[13] Here the favourable charge transfer properties of the tpphz ligand proved useful. However, in a related study for a heteroleptic ruthenium complex with carboxylated bipyridine ligands and a structurally related dipyridophenazine ligand a significant impact of the ligand composition on the photo- and electrochemistry could be observed. Most notably this complex show unexpected luminescence in water, i.e. a switch off of the known light switch effect[14,15], implying fundamentally different excited state relaxation pathways than those typically observed for complexes of this kind without anchoring groups.[16]

Phosphonate binding groups guarantee a chemically more stable link-up to semiconducting surfaces than carboxylates.[17] This general assumption has been investigated in detail in a recent publication resulting in a structure-property relationship study for $[Ru^{II}(bpy)_3]^{2+}$-derivatives differing in the quantity of phosphonate functionalized bpy ligands and the presence or absence of a CH_2-spacer between the aromatic ring and $-PO_3H_2$ anchor. T.J. Meyer *et al.* compared properties of these $[Ru^{II}(bpy)_3]^{2+}$-derivatives in solution and chemically bound on TiO_2 or ZrO_2, respectively.[17] They found that electron injection yields decrease with increased number of phosphonate substituents or the addition of a methylene spacer. But electro- and photochemical stabilities on TiO_2 are enhanced with an increasing number of phosphonate groups. In addition the binding

constants for $-CH_2PO_3H_2$ are higher compared with $-PO_3H_2$.[17] Therefrom we chose to utilize two diphosphonated bipyridine ligands including a methylene spacer. $[Ru^{II}(bpyMeP)_2tpphzPtCl_2]^{2+}$ **(4)** comprises all components of a intramolecular photocatalyst (bpyMeP = 4,4'-bis(diethyl-(methylene)phosphonate)-2,2'-bipyridine). A rutheniumpolypyridyl light harvesting unit, the bridging ligand tpphz as an electron transfer system and platinum as catalytic centre (Figure 1). As will be shown, the methyl phosphonic ester groups can be deprotected to make this complex immobilizable on SC surfaces.

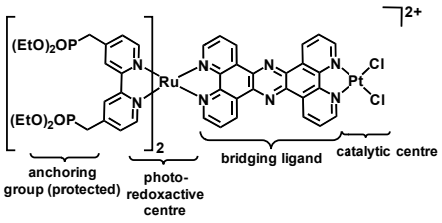

Figure 1: Desired dinuclear photocatalyst **(4)**.

(4) would be one of the first functional units which consists of a photocentre intramolecularly connected via a bridging ligand to a catalyst, which could be utilized for H_2-generation on SC surfaces. To the best of our knowledge only one other system was published yet, in which an intramolecular photocatalyst is utilized on an electrode surface.[6] However, there the assembly process of the functional catalyst is sequential, i.e. first the photoredoxactive ruthenium was bound to surface and then the catalytic active cobalt unit had to be bound to the already immobilized photocentre. Hence it was not possible to correlate the photocatalytic properties of the assembled photocatalyst on the surface with these of a molecular Ru-Co catalyst in solution. Target catalyst **(4)** would make this useful correlation feasible, since the intramolecularity of photo- and catalytic centre is given a priori. After hydrolysis of the ethyl ester groups **(4)** could be immobilized on electrode surfaces in one single step. In this contribution we describe the synthesis and photophysical and photocatalytical properties of complex **(4)**. The hydrolysis and immobilization of **(4)** are presented at the stage of preliminary tests.

Results and Discussion

Ligand Synthesis

For the composition of supramolecular systems it is necessary to apply suitable ligands which guarantee a stable linkage between the single moieties. For water reduction in an electrochemical cell the immobilization of chromophores to the SC NiO is most commonly used.[6,18,19] An effective fixation of metal complexes to NiO could be accomplished by bpyMeP as ligand.[4] The desired ligand was synthesized according to Figure S1 using modified literature methods.[20] The proton signal splitting of the methylene group between bipyridine and bromine or phosphor respectively from a singulett in 4,4'-Bis(bromomethyl)-2,2'-bipyridine to a broad duplett in bpyMeP is characteristic since it stems from the coupling of these protons with the phosphor atom. A broad coupling can also be found in ^{13}C-NMR between the methylene carbon and the phosphor atom. The ligand bpyMeP could be fully characterised by ^{1}H-, ^{13}C- and ^{31}P-NMR (([D3]MeCN, 162 MHz): δ [ppm] = 24.35), mass spectrometry (m/z (MALDI) = 457.4 $[M+1H^+)]^+$, 479.3 $[M+1Na^+)]^+$) and elemental analysis.

The structure was later confirmed by X-ray crystallography. The atom connectivity and atomic numbering scheme for bpyMeP are shown in Figure 2. Selected bond lengths and angles are given in Table 1. The structure of bpyMeP exhibits an inversion symmetry centre located on the C2-C2' bond.

Table 1: Selected bond length and angle of bpyM eP	**C1-P1**	**C1-C4**	**< C4-C1-P1**
distances / Å	**1.791**	**1.507**	**-**
angle / °	**-**	**-**	**115.7**

The C-N-C angle of 116.9° within the pyridine ring is similar to those for free pyridine (for example, about 117° in a pyridine derivative[21]).The two pyridyl rings within bpyMeP are in anti conformation with no deviation from planarity.

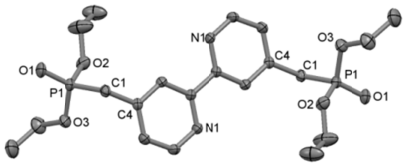

Figure 2: Solid-state structure of bpyMeP. Hydrogen atoms are omitted for clarity.

The C1-P1 bond is turned out of the bipyridine plane with a torsion angle of 88.17°. The bond length between C4 in the pyridine ring and the methylene C1 is given as 1.507 Å and is therefore in the normal range of a sp^3-C-sp^2-C single bond. Likewise the C1-P1-distance exhibits a standard value of 1.791 Å for a methylene C – phosphonate P – bond. Neither hydrogen bonding nor π-π-stacking were found within the structure.

Metal Complex Synthesis

Here we present the synthesis of the mono- and dinuclear target complexes $[Ru^{II}(bpyMeP)_2tpphz]^{2+}$ **(3)** and $[Ru^{II}(bpyMeP)_2tpphzPtCl_2]^{2+}$ **(4)** (Figure 3).

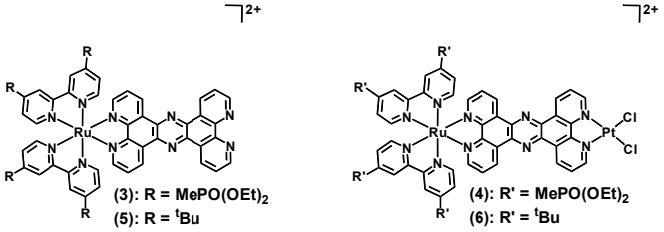

Figure 3: Structures of Ru-complexes **(3)**, **(4)**, **(5)**, **(6)**.

The coordination of one bpyMeP-ligand to a Ru^{2+} core was already described by Odobel and coworkers in 2001 with the complex $[Ru^{II}(bpy)_2(bpyMeP)]^{2+}$.[20] To assure comparability to complexes **(3)** and **(4)** within this contribution we synthesized $[Ru^{II}(tbbpy)_2(bpyMeP)]^{2+}$ **(M)** as a model complex with more electron-rich bipyridines. The synthesis of **(M)** was accomplished by reaction of $[Ru^{II}(tbbpy)_2Cl_2]$ with one equivalent of bpyMeP in an ethanol/water-mixture for 20h. **(M)** was characterised by ^{1}H-, and ^{31}P-NMR (([D3]MeCN, 162 MHz): δ [ppm] = 23.00). The solid-state structure of **(M)** was derived from X-ray suitable single crystals which were grown by slow vapor diffusion of diethyl ether into a solution of the complex in acetone (Figure 4).

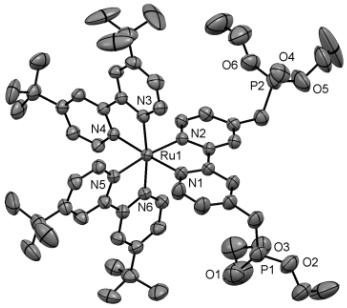

Figure 4: Solid-state structure of the complex cation of **(M)** (ellipsoids at 50% probability; solvent molecules, anions and hydrogen atoms omitted for clarity)

Upon coordination phosphonic ester groups are turned into cis configuration with respect to the C2-C2'-bond of the bipyridine. No significant changes are observed considering the pyridine-C-methylene-C bond, the methylene-C-P bond, or the respective angle <(CCP) (cf. Table 2).

Table 2: Selected bond length and angle of **(M)**	C_{me}-P	C_{py}-C_{me}	< C_{py}-C_{me}-P
distances[a] / Å	**1.781**	**1.505**	**-**
	1.788	**1.513**	**-**
angles[a] / °	**-**	**-**	**110.2**
	-	**-**	**113.3**

[a]with respect to the two phosphonate groups being symmetrically non-equivalent in the complex

The Ru-N bond lengths (2.051(3) Å – 2.067(3) Å) and bite angles (78.5° - 79.0°) of all bipyridine ligands are in the usual range.

The coordination of two bpyMeP-ligands to a Ru^{2+} core should provide four anchoring groups per ruthenium complex, ensuring stable binding on semiconductor-surfaces. The preparation of complex **(1)** with L,L' = Cl as a precursor is literature known. But the yields did not surpass 32%.[22] Hence different preparation routes were investigated to optimize the yield of **(1)**. bpyMeP turned out to be instable in a microwave-assisted reaction with $Ru[(COD)Cl_2]_n$ which is usually used for the efficient synthesis of $(bpy)_2RuCl_2$-derivatives.[23] Also a two steps synthesis of **(1)**, starting with refluxing $Ru[(CO)_2Cl_2]_n$ and one equivalent of bpyMeP in MeOH then introducing the second equivalent by lightdriven reaction failed.[24,25] The coordination of two equivalents of bpyMeP to Ru finally was accomplished by using $Ru(DMSO)_4Cl_2$ as precursor in methanol with a reaction time of 20 h at reflux. Looking at previous results, the reaction of two bpy-like ligands with $Ru(DMSO)_4Cl_2$ might lead to Ru complexes with different substitution patterns. DMSO as well as Cl could be replaced bpy.[26,27] Since the substitution pattern of **(1)** (Cl or DMSO) is not important for the preparation of **(2)** or other $[Ru^{II}(bpyMeP)_2L]^{2+}$ -complexes the raw product was used directly without further purification for the next step (Figure 5).

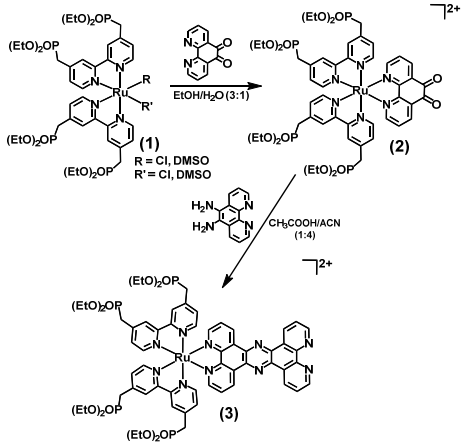

Figure 5: Synthesis of **(2)** and **(3)**.

The $Ru(bpyMeP)_2Cl_{2-x}/DMSO_x$-complexes are refluxed with an equimolar amount of $phen(O)_2$ (1,10-Phenanthrolin-5,6-dione) in an ethanol/water mixture for 20 h. Starting with $Ru(DMSO)_4Cl_2$ the overall yield of **(2)** is 86%. Hence this synthetic route proved itself as a high-yielding methode to generate $[Ru^{II}(bpyMeP)_2L]^{2+}$ -complexes.

Recently T.J. Meyer *et al*. published another approach to synthesize $[Ru^{II}(bpyMeP)_2L]^{2+}$ with L = bpy.[28] They applied a $[Ru(\eta^6\text{-}C_6H_6)(bpy)OTf]OTf$ precursor with two equivalents of bpyMeP in 1:1 (v/v) $EtOH/H_2O$ under refluxing conditions to generate the hydrolyzed form of $[Ru^{II}(bpyMeP)_2bpy]$ in 62% yield. In other words, they first introduced bpy and in a second step two equivalents of bpyMeP to the Ru^{2+} core. The preparation of **(3)** would therefore imply the generation of the precursor $[Ru(\eta^6\text{-}C_6H_6)(tpphz)OTf]OTf$**.** Since a successful synthesis of this precursor is intricate and the synthesis of **(2)** by our presented procedure is straight forward and high yielding, we decided to avoid this alternative strategy.

Beginning with **(2)** and $phen(NH_2)_2$ (1,10-Phenanthrolin-5,6-diamine) the synthesis of **(4)** is performed by two steps. At first the bridging ligand tpphz is synthesized by condensation of $phen(NH_2)_2$ and $phen(O)_2$ to yield **(3)**. In principle this condensation in the presence of a coordinated Ru-complex is known to literature.[29] A direct introduction of the poorly soluble tpphz to **(1)** was avoided because of the thermal instability of bpyMeP under high-temperature conditions needed for the introduction of tpphz.[7] Our best results for the tpphz-condensation were obtained by working in an acetonitrile/glacial acetic acid mixture (4:1) under inert atmosphere. After work up by column chromatography and recrystallisation **(3)** was received in 57% yield and characterised by ^{1}H-, ^{13}C-, ^{31}P-NMR (([D3]MeCN, 162 MHz): δ [ppm] = 22.92), mass spectrometry (m/z (MALDI/TOF) = 699.50 $[(M\text{-}2PF_6)/2]^{2+}$, 1543.42 $[M\text{-}PF_6]^+$.) and elemental analysis. To complete the photocatylst **(4)** Pt has to be coordinated to the free phenanthroline sphere of tpphz. For this purpose **(3)** and $Pt(DMSO)_2Cl_2$ are refluxed in ethanol for 5 h to gain **(4)** in 82% yield. The target complex **(4)** was characterised by ^{1}H-, ^{31}P-NMR (([D3]MeCN, 162 MHz): δ [ppm] = 22.82), mass spectrometry (m/z (MALDI/TOF) = 832.65 $[(M\text{-}2PF_6)/2]^{2+,}$ 1809.28 $[M\text{-}PF_6]^+$) and elemental analysis. If one compares the ^{31}P-NMR shifts of bpyMeP with **(3)** and **(4)** there is almost no difference, indicating that the coordination to mono- or dinuclear ruthenium complexes has minor electronical effects on the phosphor atoms of bpyMeP. The introduction of Pt to **(3)** tpphz could be observed by ^{1}H-NMR-spectroscopy. As known from previous investigations the ^{1}H-NMR signal shifts of similar Ru-complexes like **(3)** and **(4)** are concentration dependent.[30,31] For comparison it must be guaranteed that the spectra are measured at equivalent concentrations. The

presence of Pt leads to a decreasing electron density at the tpphz moiety. This deshielding has a particularly strong effect on the protons which are located in direct proximity of Pt. In comparison to **(3)** their signals are shifted to downfield (cf. protons a' in Figure S3 in the SI.)

Photophysics

Absorption spectra for **(3)** and **(4)** in MeCN (measured at a concentration of 10^{-5} M) (Figure 6) exhibit characteristic intense π–π* absorptions below 350 nm and metal-to-ligand charge-transfer (MLCT) absorptions from 400 to 500 nm as usual for ruthenium polypyridyl complexes.[32] Both compounds feature a similar MLCT absorption maximum ($\lambda_{max} \approx 450$ nm). Notably **(4)** does not reveal the pronounced absorption bands which **(3)** shows at 380 nm. These bands are assigned to phenanzine based π-π*-transitions. As previously shown, these absoptions features are also absent in structurally related Ru-tpphz-Pt complexes.[33] Thus, the absorption spectrum presents a strong indication for the coordination of platinum on the free phenanthroline sphere of tpphz in **(4)**. This is assured by the quenching of the emitting excited state by platinum as shown in the emission spectra (Figure 6).[12] Complex **(3)** shows the light switch effect. Typically the luminescent state is active in aprotic solvents whereas the non-luminescent state dominates in protic solvents such as water. As depicted in Figure S4 in the SI the luminescence of **(3)** is quenched by adding water to the MeCN dye solution. So **(3)** shows the expected photophysical properties of similar Ru-tpphz-complexes and the methyl phosphonic ester groups do not change the emission behavior compared to related compounds without anchoring groups.[34,35] This is in contrast to related Ru-dppz complexes with dicarboxylated bipyridines for which no such light switch effect could be observed.[16] From these results one can infer that the photophyisical properties of **(3)** are not changed significantly if methyl phosphonic ester groups are utilized as anchoring groups.

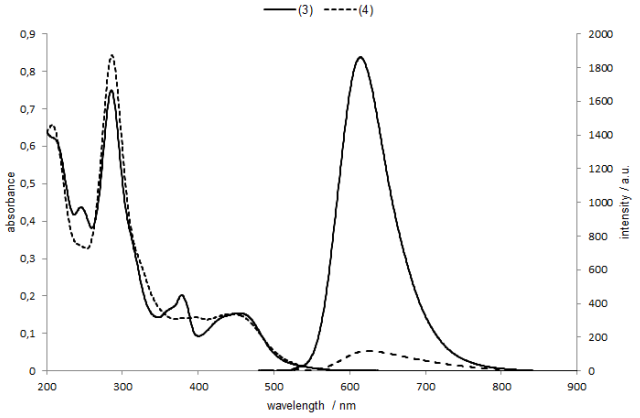

Figure 6: UV/Vis and emission spectra of **(3)** and **(4)**.*
*= identical excitation conditions for measuring the emission spectra of **(3)** and **(4)** at identical optical density at 459 nm.

Absorption and emission spectra of **(3)** and $[Ru^{II}(tbbpy)_2tpphz]^{2+}$ **(5)** after excitation within the range of the MLCTs were recorded at a dye concentration of 5 $x10^{-6}$ M. The comparison of **(3)** with **(5)**, where the bpyMeP ligands are replaced by tbbpy, shows different absorption and emission characteristics, which point to altered excited state properties upon introduction of the bpyMeP ligand (cf. Figure S5 in the SI.) (tbbpy=4,4'-bis(*t*butyl)-2,2'-bipyridine). Concerning the absorption, **(3)** exhibits a pronounced maximum at low energy part of MLCT band (bathochromic shift of 646.4 cm^{-1}, i.e. 0.08 eV compared to **(5)**) whereas in the emission spectrum a slight hypsochromic shift could be observed (513.8 cm^{-1}, i.e. 0.064 eV compared to **(5)**). This antipodal behavior leads to a difference in Stokes shifts of **(5)** compared to **(3)** obviously caused by the exchange of bpy substituents. The bathochromic shift in absorption could be explained by the electron-withdrawing substituent effect of the methyl phosponic ester groups in lowering the π* levels on bpyMeP with respect to tbbpy as similarly described by T.J.Meyer et al.[28] This electron-pull induces also a lowered electron density at the Ru centre of **(3)** in comparison to the Ru centre of **(5).** This might be an explanation for the hypsochromic shift in emission. Important absorption and emission features of complexes **(2)** - **(5)** are summarized in Table 3.

Table 3: Absorption and emission data of complexes **(2)** - **(5)** measured in acetonitrile (MLCT absorption maxima λ_{MLCT}; phenazine based transition maxima λ_{phz}; emission maxima λ_{em})

Substance	λ_{MLCT} [nm]	λ_{phz} [nm]	λ_{em} [nm]
(2)	**443**	**-**	**614**
(3)	**455**	**381**	**614**
(4)	**445.5**	**-**	**624**
(5)	**442**	**381.5**	**635**

Electrochemical Properties

In order to study the effect of the phosphonate ester moiety on the electronic properties of the Ru-centre, related mononuclear complexes are investigated. The redox potential for the $Ru^{III/II}$ couple in **(3)** occurs at more positive potential than that of the $Ru^{III/II}$ of **(5)** (cf. Table 4, Figure S6 in the SI). The *t*butyl-groups are more electron-donating compared to methyl phosphonic ester substituents, resulting in an eased oxidation of Ru^{II} in **(5)**. If compared to $[Ru^{II}(bpy)_2tpphz]^{2+}$ with unsubstituted and $[Ru^{II}(bpy(COOMe)_2)_2dppz]^{2+}$ with carboxylic ester substituted bpy ligands Ru^{II} oxidation becomes easier in the following order: $[Ru^{II}(bpy(COOMe)_2)_2dppz]^{2+}$ < **(3)** < $[Ru^{II}(bpy)_2tpphz]^{2+}$ < **(5)**.[16,36] In the same order the character of peripheral bpy substitutent changes from electron withdrawing to electron donating.

Table 4: Electrochemical data for complexes of the types Rutpphz and Ruddpz.

Substance	Half-Wave Potentials E (V) for the Oxidation $E_{1/2}(Ru^{III}/Ru^{II})$[a]
(3)[b][d]	**1.02**
(5)[b][d]	**0.86**
$[Ru^{II}(bpy)_2tpphz]^{2+}$[b][e]	**0.93**
$[Ru^{II}(bpy(COOMe)_2)_2dppz]^{2+}$[c][f]	**1.14**

[a] The electrochemical measurements were carried out in anhydrous and argon purged MeCN.
[b] 0.1 M NBu_4PF_6 as supporting electrolyte.
[c] 0.1 M NBu_4ClO_4 as supporting electrolyte.
[d] the oxidation potentials are given vs. Fc/Fc^+.
[e] from reference [36]; Fc/Fc+ = + 0.40 V vs. SCE in acetonitrile
[f] from reference [16]; Fc/Fc+ = + 0.36 V vs. Ag/AgCl in acetonitrile

Resonance-Raman-Experiments

The localization of the initially excited state (Franck-Condon-point) is highly important for the catalytic process as has been shown before for the ruthenium/palladium dyad $[Ru(tbbpy)_2tpphzPdCl_2]^{2+}$.[37] For $[Ru(tbbpy)_2tpphzPdCl_2]^{2+}$excitation the red-edge of the ^{1}MLCT absorption band - populates a mainly tpphz-based state which can be deactivated via vectorial electron transfer to the Pd centre. [8,9] The discussed electron-withdrawing properties (*vide supra*) of the bpyMeP ligands may, however, result in a different Franck-Condon-point structure. It was therefore of immediate interest to determine the localization of the initially excited state on certain parts (bridge or periphery) of compound **(4)**. Resonance-Raman spectroscopy is suited to investigate the localization of states shortly after excitation due to the enhancement of modes that display a large nuclear displacement from the equilibrium geometry at the Franck–Condon point.[38] We recorded resonance-Raman spectra of **(3)** and **(4)** in MeCN solution upon excitation at 458, 476 and 514 nm, *i.e.* in resonance with the ^{1}MLCT-absorption of the complexes. Resonance-Raman spectra at

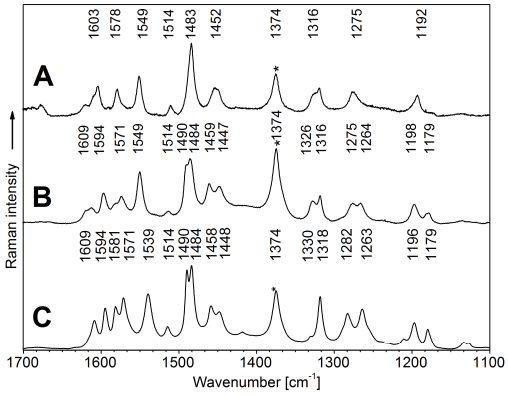

Figure 7 gives a comparison between the resonance-Raman spectra (λ_{exc} = 458 nm) of the Ru-complex (3) (spectrum A), the Ru/Pt complex (4) (spectrum B) and the previously published $[Ru(tbbpy)_2tpphzPdCl_2]^{2+}$ (spectrum C) in acetonitrile solution.[37] The solvent band at 1374 cm^{-1}is marked with an asterisk.

514 nm suffer from a strong luminescence background and are therefore not displayed. The resonance-Raman spectra obtained for excitation of **(4)** at 458 nm show modes from the peripheral bpyMeP ligands as well as from the tpphz-bridge (Figure 7).

The spectrum of **(4)** closely resembles that of the previously reported $[(tbbpy)_2RutpphzPdCl_2]^{2+}$.[37] Comparison between **(4)** and $[Ru(tbbpy)_2tpphzPdCl_2]^{2+}$ shows that the relative signal intensities are not changed significantly. Only two bands of **(4)** appear at different positions than those of $[Ru(tbbpy)_2tpphzPdCl_2]^{2+}$ (**(4)**: 1549, 1275 cm^{-1}; $[Ru(tbbpy)_2tpphzPdCl_2]^{2+}$: 1539, 1282 cm^{-1}). The latter were previously assigned to the peripheral ligands, the structure of which is directly impacted by introduction of the anchoring group.[9] Resonance-Raman experiments are suited to gain information about the energetic order of different electronic transitions that compose a UV/Vis band. This is achieved by a comparison of the resonance-Raman spectra obtained from excitation at different energies of the UV/Vis band. A comparison between the resonance-Raman spectra obtained by excitation of **(4)** at 458 nm and 476 nm respectively, reveals that the relative intensities of the bipyridine marker bands (at 1547, 1484, 1318 cm^{-1}) decrease compared to the tpphz bands when going from higher to lower energy (458 nm to 476 nm, Figure S7, Supporting Information). The same observation was made for **(3)** (Figure S8, Supporting Information). This indicates that the low energy flank of the ^{1}MLCT absorption band is governed by $^1MLCT_{tpphz}$←GS charge transfer while the higher energy side is governed by $^1MLCT_{bpyMeP}$←GS transitions (GS is ground state).
From this comparison we conclude that changing the peripheral ligands from 4,4'-bis(*t*butyl)-2,2'-bipyridine to 4,4'-bis(diethyl(methylene)phosphonate)-2,2'-bipyridine does not alter the localization of the initially photoexcited state. This is relevant for an efficient catalytic process, independent of the nature of the catalytic metal centre (palladium or platinum).

Catalysis:

The new heterodinuclear ruthenium complex $[Ru^{II}(bpyMeP)_2tpphzPtCl_2]^{2+}$ **(4)** was investigated towards its catalytic activity for light-driven hydrogen production and compared to $[Ru^{II}(tbbpy)_2tpphzPtCl_2]^{2+}$ **(6)**. Therefore commercially available LED sticks (λ=470 nm, P=45 mW) in combination with a specialized air-cooled photomicroreactor were used. Irradiation times of 72 h or 17 h, respectively, were recorded in the presence of triethylamine (TEA) acting as a sacrificial electron donor. For both complexes, the catalytic activity is higher in the presence of water (10 vol.%). This is in accordance with similar RutpphzPd complexes where water has an optimal concentration range between 10 and 15 vol.% and already minor amounts of water strongly increase catalytic activity up to a turnover number of 210 for $[Ru^{II}(tbbpy)_2tpphzPdCl_2]^{2+}$.[8] Higher water concentrations are limiting the catalytic turnover. Possibly this is associated with the disadvantageous effect of water on the long-lived excited state in ruthenium complexes bearing a phenazine moiety.[39] To ensure comparability the catalyst concentration (c = 7x10^{-5} mol/L) were kept constant. **(4)** and **(6)** show no induction phase, indicating that they are really the active catalyst. In contrast to RutpphzPd where an significant induction period was observed, suggested to be related to the photodecomposition and formation of colloidal intermediates.[10] The period of active catalysis of the RutpphzPt catalyst is prolonged by replacing tbbpy with bpyMeP from 10h for **(6)** to 48h for **(4)**. As can be seen, **(4)** displays a generally higher turnover number (TON) than **(6)** (37 vs. 7) (Figure 8). One possible reason for the improved catalytic activity of **(4)** could be due to the increased energy of the luminescent state detected for **(3)** if compared to **(5)**, as described above. Furthermore, the phosphonate moieties represent significantly more polar groups than the *t*butyl-groups in **(6)**. They may therefore lead to a different aggregation of the catalyst thus providing more optimal conditions for proton migration and activation. As shown for RutpphzPd-complexes, optimization of the supramolecular aggregation in solution can have a significant effect on the catalytic activity.[40] As described above **(4)** with $PtCl_2$ as catalytic unit shows lower catalytic turnover than similar complexes with $PdCl_2$. However, its utilization as an intramolecular photocatalyst on semiconducting surfaces seems more appropriate, since colloid formation, which goes along with the loss of the intramolecular character, can be excluded.

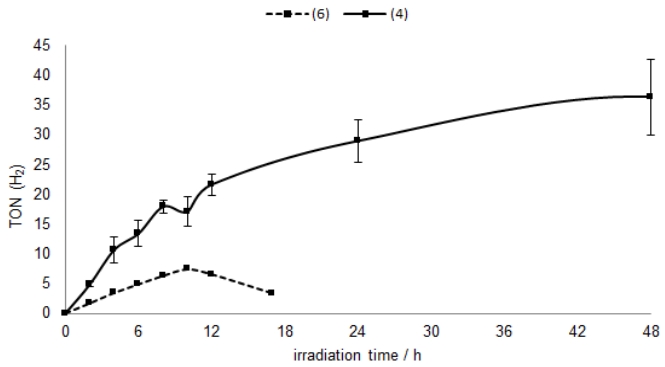

Figure 8: Photocatalytic activity of **(4)** and **(6)**.

Hydrolysis and Immobilization

In order to investigate principle utilisability of the presented compounds **(3)** and **(4)** in dye sensitized cells, preliminary investigations into deprotection and immobilization were performed. The methyl phosphonic ester groups of model complex $[Ru^{II}(tbbpy)_2bpyMeP]$ **(M)** were deprotected by reaction half-concentrated HCl at reflux as reported for a similar complex by Odobel and coworkers.[20] The loss of the ethylgroups of **(M)** can be traced by ^{1}H-NMR spectroscopy (Figure S10, Supporting Information). The deprotected species $[Ru^{II}(tbbpy)_2(bpy(CH_2PO_3H_2)_2)]^{2+}$ **($M_{hydrolyzed}$)** is soluble in water (most probably as Cl^--salt) and can be reprecipitated as PF_6-salt to regain solubility in organic solvents. Comparison of the ^{31}P-NMR-spectra in acetonitrile of **(M)** and its deprotected analogue **($M_{hydrolyzed}$)** revealed only minor change in the chemical shift with δ [ppm] = 23.00 and δ [ppm] = 19.22, respectively. Notably, deprotection of **(3)** and **(4)** according to the above described procedure yielded completely insoluble products.
However, addition of NaOH rendered the deprotected compounds **(3)** and **(4)** water-soluble, most probably as 6-fold negatively charged species. Unfortunately the ^{1}H-NMR spectra of these complexes in D_2O + 4% NaOD show complicated shapes compared to the protected species which were not straight-forward to interpret. But in the ^{31}P-NMR-spectra signals similar to the one for **($M_{hydrolyzed}$)** in deuterated water could be found (δ [ppm] = 14.77 for **(3)** and **(4)** compared to δ [ppm] = 14.74 for **($M_{hydrolyzed}$)**, cf. Figure S11 in the SI). The other signals at around 15 ppm might be explained by differing degrees of deprotonation of **($3_{hydrolyzed}$)** or **($4_{hydrolyzed}$)** respectively. The presence of these different species might also be the reason for the complex ^{1}H-NMR spectra. In contrast to **($M_{hydrolyzed}$)** a signal at ca. 5.5 ppm was found for **($3_{hydrolyzed}$)** and **($4_{hydrolyzed}$)**. One possible explanation for its appearance is the coordination of Na^+-ions at the phosphonate groups of **($3_{hydrolyzed}$)** and **($4_{hydrolyzed}$)**, resulting in an downfield shift as observed for (benzoxazol-2-ylmethyl)phosphonic acid for instance.[41] In the absorption spectra no significant changes could be monitored when comparing **(M)**, **(3)** and **(4)** in acetonitrile to their hydrolyzed analogue **($M_{hydrolyzed}$)**, **($3_{hydrolyzed}$)** and **($4_{hydrolyzed}$)** in water (cf. Figures S12 – S14 in the SI). The complexes **($M_{hydrolyzed}$)**, **($3_{hydrolyzed}$)** and **($4_{hydrolyzed}$)** were immobilized on a NiO surface on a FTO glass carrier by dipping the NiO substrate for 3 days into a 0.2 mM solution of **($M_{hydrolyzed}$)**, **($3_{hydrolyzed}$)** and **($4_{hydrolyzed}$)** in 0.1M NaOH, after using the deprotection method described above. The sensitized NiO films were washed several times with water and then analyzed by UV/Vis (reflection spectroscopy) in the MLCT region. For all complexes no significant changes in absorption behavior were found when comparing the protected, the hydrolyzed and the immobilized species (cf. Figures S12 - S14 in the SI). **(3)@NiO** shows the phenanzine based π-π*-transitions band at 370 nm (Figure 9, cf. Figure 6) whereas **(4)@NiO** still shows the characteristic unstructured absorption behavior typical for the RutpphzPt-species. For both films the MLCT absorption band ($\lambda_{max} \approx 450$ nm) of complexes **(3)** and **(4)** can be observed.

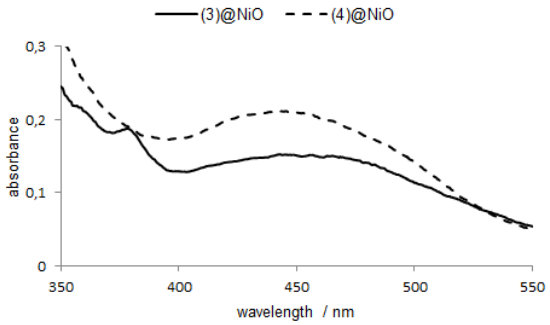

Figure 9: UV/Vis (reflection) spectra of immobilized **($3_{hydrolyzed}$)** and **($4_{hydrolyzed}$)** on **NiO@FTO** glass.**
= NiO and FTO glass background **substracted

Experimental

Methods and materials

^{1}H (400.13 MHz), ^{13}C-NMR (101 MHz) and ^{31}P (161.98 MHz) spectra were measured with a Bruker DRX 400 spectrometer. The NMR spectra were recorded in CD_3CN or $CDCl_3$ at 298 K. ^{1}H-NMR chemical shifts were referenced to the solvent peak for acetonitrile (δ = 1.94 ppm) or chloroform (δ = 7.26 ppm).

MS analysis was performed on Bruker solariX (2010) Hybrid 7T FT-ICR for MALDI and with a Bruker Ultraflex III MALDI TOF/TOF for MALDI/TOF measurements.

The crystal suitable for X-ray analysis was mounted using a MicroLoop and Fomblin oil. X-ray diffraction intensity data were measured at 180 K on a SuperNova (Dual Source) diffractometer, equipped with an ATLAS detector, from Agilent Technologies. The structures were solved by direct methods (SHELXS) and refined by full-matrix least squares techniques against Fo2 (SHELXL 2013).[42] The hydrogen atoms were included at calculated positions with fixed thermal parameters. All non-hydrogen atoms were refined anisotropically.

Electrochemical data were obtained by cyclic voltammetry using a conventional single-compartment three-electrode cell arrangementin combination with a "Parstat 2273 Princeton Applied Research" potentiostat. The measurements were carried out in 0.1M solutions of Bu_4NPF_6 in dry and argon purged acetonitrile. All values were determined with a glassy carbon working electrode and platinum counter and reference electrodes. The measured values were referenced versus the redox couple Fc/Fc^+ set at $E_{1/2} = 0$V.

The hydrogen evolved was measured by headspace GC on a Bruker Scion GC/MS, with a thermal conductivity detector 15 (column: Mol. Sieve 5A 75m x 0.53 mm I.D., oven temp. 70 °C, flow rate 22.5 ml/min, detector temp. 200 °C) with argon as carrier gas. The GC was calibrated by mixing different volumes of pure hydrogen together with argon into a schlenk vessel. The obtained signal was plotted against the calibration curve and 20 multiplied accordingly to receive the total produced hydrogen content in the headspace.

The UV/Vis-spectra were recorded with a JASCO Spectrometer V-670. Quartz cells with a 10 mm path length were used.
The emission-spectra were recorded with a JASCO 25 Spectrofluorometer FP-8500. Quartz cells with a 10 mm path length were used.

Immobilization of the hydrolyzed complexes on a NiO surface on a FTO glass carrier was accomplished by dipping the NiO substrate for 3 days at 20 °C into a 0.2 mM solution of the dye in 0.1M NaOH. After immobilization the dye sensitized NiO films were washed several times with water.

If not mentioned otherwise all experiments were performed under aerobic conditions.

Starting materials

4,4'-Dimethyl-2,2'-bipyridine and ruthenium trichloride trihydrate ($(RuCl_3 \cdot 3H_2O)$ was purchased from commercial sources and used without further purification. $Ru[DMSO]_4Cl_2$, $[Ru^{II}(tbbpy)_2Cl_2]$, $[Ru^{II}(tbbpy)_2(tpphz)](PF_6)_2$ **(5)** and $[Ru^{II}(tbbpy)_2(tpphz)PtCl_2](PF_6)_2$ **(6)** were preapared as reported elsewhere.[7,23,43,11]

Ligand Synthesis

4,4′-Dicarboxy-2,2′-bipyridine

This compound was prepared as previously reported.[44]

4,4′-Diethoxycarbonyl-2,2′-bipyridine

This compound was prepared as previously reported.[20]

4,4′-Dicarboxyethyl Ester 2,2′-bipyridine

This compound was prepared by a modified literature procedure.[20] An 5.5 g amount of sodium borohydride was added to a mixture of 4,4′-Diethoxycarbonyl-2,2′-bipyridine (5.0 g, 16.7 mmol) in 400 mL of degased isopropyl alcohol. The mixture was refluxed for 24 h and cooled to room temperature, and then another 5.5 g portion of sodium borohydride was added. After another 36 h heating at reflux the solvent was removed under vacuum and the residue was dissolved in a small amount of water.The resulting solution was extracted with ethyl acetate (3 x 200 mL), dried over magnesium sulfate, and the solvent was removed under vacuum. The desired solid was obtained in 86% yield. Characterization data match literature values.[20]

4,4′-bis(bromomethyl)-2,2′-bipyridine

This compound was prepared as previously reported.[20]

4,4′-bis(diethyl(methylene)phosphonate)-2,2'-bipyridine (bpyMeP)

This compound was prepared as previously reported.[20]
^{1}H-NMR ([D3]MeCN, 400 MHz): δ [ppm] = 8.59 (d, 2H, ^3J *(H,H)* = 4.8 Hz), 8.31 (s, 2H), 7.30 (m, 2H,), 4.05 (q, 8H, ^3J *(H,H)* = 7.2 Hz), 3.21 (d, 4H, ^2J *(H,P)* = 22.4 Hz), 1.25 (t, 8H, ^3J *(H,H)* = 7.2 Hz); ^{13}C-NMR ([D3]MeCN, 101 MHz):): δ ppm = 156.00, 149.23, 142.15, 124.96, 122.50, 62.40, 33.57 (^1J *(H,P)* = 137.4 Hz), 16.35.; ^{31}P-NMR ([D3]MeCN, 162 MHz): δ ppm = 24.35; MS (MALDI): m/z = 457.4 $[M+1H^+)]^+$, 479.3 $[M+1Na^+)]^+$; elemental analysis calcd. (%) for $C_{20}H_{30}N_2O_6P_2$: C = 52.63, H = 6.63, N = 6.14; found: C = 51.85, H = 6.52, N = 6.02.

Crystals suitable for X-ray analysis were obtained by slow evaporation of chloroform.

Crystal data: $C_{20}\ H_{30}\ N_2\ O_6\ P_2$, M_r = 456.40 g mol^{-1}, colourless prism, crystal size 0.213 x 0.158 x 0.088 mm^3, triclinic, space group *P* -1, a = 7.3747(3) Å, b = 8.5221(4) Å, c = 9.7222(6) Å, α = 97.051(4)°, β = 97.098(4)°, γ = 107.244(4), V = 570.84(5) Å^3, T = 180(2) K, Z = 2, $\rho_{calcd.}$ = 1.328 Mg/m3, μ (Cu-Kα) = 2.058 mm^{-1}, F(000) = 242, altogether 5287 reflexes up to h(-8/9), k(-10/10), l(-12/11) measured in the range of 7.801° ≤ Θ ≤ 73.042° , completeness Θ_{max} = 99.6 %, 2215 independent reflections, R_{int} = 0.0139, 2130 reflections with Fo > 4 σ(Fo), 138 parameters, 0 restraints, $R1_{obs}$ = 0.0383, $wR2_{obs}$ = 0.1033, $R1_{all}$ = 0.0393, $wR2_{all}$ = 0.1044, GOOF = 1.015, largest difference peak and hole: 0.769/-0.466 e·Å^{-3}. CCDC 1021494 contains the supplementary crystallographic data for this paper. These data can be obtained free of charge from The Cambridge Crystallographic Data Centre via www.ccdc.cam.ac.uk/data_request/cif.

Metal Complex Synthesis and Characterization

$[Ru^{II}(bpyMeP)_2Cl_x/DMSO_{2-x}]$ (1)

A solution of 4,4′-Bis(diethyl(methylene)phosphonate)-2,2'-bipyridine (0.80 g, 1.75 mmol) and $Ru[DMSO]_4Cl_2$ (0.42 g, 0.88 mmol) are refluxed in methanol for 24 h. During this time the color changed from yellow to dark brown. After removal of methanol at the rotary evaporator the residue was dissolved in a little ethanol. An excess of diethyl ether was added to the solution. The resulting brown precipitate was collected and dried. This crude product was used in the next reaction without further purification.

$[Ru^{II}(bpyMeP)_2(phen(O_2))](PF_6)_2$ (2)

A solution of **(1)** (0.80 g, 709.6 μmol) and 1,10-Phenanthroline-5,6-dione (149.1 mg, 709.6 μmol) are refluxed in an ethanol/water mixture (30 mL/10 mL) for 20 h. During this time the color changed from deep brown to dark red. After removal of most of the ethanol at the rotary evaporator an excess of NH_4PF_6 was added to the solution The resulting red precipitate was collected, washed with water and diethyl ether and dried (86% yield starting with $Ru[DMSO]_4Cl_2$).

^{1}H-NMR ([D3]MeCN, 400 MHz): δ [ppm] = 8.54 (dd, 2H, ^4J *(H,H)* = 1.3 Hz, ^3J *(H,H)* = 8 Hz), 8.46 (s, 2H), 8.43 (s, 2H), 7.99 (dd, 2H, ^4J *(H,H)* = 1.3 Hz, ^3J *(H,H)* = 5.6 Hz), 7.76 (m, 2H, ^3J *(H,H)* = 5,8 Hz), 7.67 (m, 2H), 7.44-7.34 (m, 6H), 4.03 (m, 16H), 3.48-3.37 (m, 8H), 1.23-1.12 (m, 24H); ^{31}P-NMR ([D3]MeCN, 162 MHz): δ [ppm] = 22.83, 22.74.

$[Ru^{II}(bpyMeP)_2(tpphz)](PF_6)_2$ (3)

(2) (0.20 g, 0.154 mmol) was dissolved in a mixture of acetonitrile/glacial acetic acid (150 mL/40 mL) and degased with argon for 30 min. Then the first equivalent of 1,10-Phenanthroline-5,6-diamine ($phen(NH_2)_2$, 106.2 mg, 505.3 μmol) was added to the solution. After 6 h of boiling to reflux under an argon atmosphere a second equivalent of 1,10-phenanthroline-5,6-diamine ($phen(NH_2)_2$, 106.2 mg, 505.3 μmol) was added and the red solution was heated for a further 12 h. After cooling the reaction mixture was filtered. Most of the solvent was removed using rotary evaporation and NH_4PF_6 was added, resulting in the formation of a precipitate which was collected, washed well with water, diethyl ether and dried in vacuo. The solid was purified using a gradient chromatography changing from acetonitrile–water (8/2) to acetonitrile–water/KNO_3. Recrystallization in ethanol yielded in the formation of a red powder (57%).

^{1}H-NMR ([D3]MeCN, 400 MHz): δ [ppm] = 9.70 (d, 2H, ^3J *(H,H)* = 7.6 Hz), 9.46 (d, 2H, ^3J *(H,H)* = 8 Hz), 8.69 (s, 2H), 8.45 (s, 2H), 8.40 (s, 2H), 8.20 (d, 2H, ^3J *(H,H)* = 5.2 Hz), 7.92 (m, 2H), 7.84 (m, 2H), 7.80 (m, 2H), 7.73 (d, 2H, ^3J = 6 Hz), 7.38 (d, 2H, ^3J *(H,H)* = 5.6 Hz), 7.22 (d, 2H, ^3J *(H,H)* = 5.6 Hz), 4.00 (m, 8H), 3.85 (m, 8H), 3.40 (dd, 4H, ^2J *(H,P)* = 22.8 Hz), 3.29 (dd, 4H, ^2J *(H,P)* = 22.8 Hz), 1.15-0.95 (m, 24H); ^{13}C-NMR ([D3]MeCN, 126 MHz): δ [ppm] = 157.10, 156.19, 153.90, 153.69, 152.41, 151.42, 149.77, 147.12, 145.32, 144.89, 144.82, 140.11, 138.08, 133.22, 129.05, 128.98, 128.70, 127.01, 125.77, 125.29, 125.08, 124.72, 62.52, 62.28, 33.22 (^1J *(H,P)* = 133.6 Hz), 33.07 (^1J *(H,P)* = 134.8 Hz), 15.79, 15.60.; ^{31}P-NMR ([D3]MeCN, 162 MHz): δ [ppm] = 22.92.; MS (MALDI): m/z = 699.50 $[(M-2PF_6)/2]^{2+}$, 1543.42 $[M-PF_6]^+$; elemental analysis calcd. (%) for $C_{64}H_{72}F_{12}N_{10}O_{12}P_6Ru$: C = 45.53, H = 4.30, N = 8.30; found: C = 44.57, H = 4.56, N = 7.99.

$[Ru^{II}(bpyMeP)_2(tpphz)PtCl_2](PF_6)_2$ (4)

A red solution of **(3)** (100 mg 59.2 µmol) and $Pt(DMSO)_2Cl_2$ (30 mg, 71 µmol) are refluxed in 60 mL ethanol for 5 h. During that time the color of the solution changed to dark red. A good portion of the ethanol is removed and an aqueous solution of NH_4PF_6 added. The resulting solid was isolated by filtration, washed well with water and diethylether. Subsequent drying in vacuo resulted in a dark red solid (82% yield).

^{1}H-NMR ([D3]MeCN, 400 MHz): δ [ppm] = 9.81 (d, 2H, ^3J *(H,H)* = 8.4 Hz), 9.36 (d, 2H, ^3J *(H,H)* = 8 Hz), 9.15 (s, 2 H), 8.50 (s, 2H), 8.47 (s, 2H), 8.37 (d, 2H, ^3J *(H,H)* = 5.2Hz), 8.06 (m, 2H), 8.02 (m, 2H), 7.94 (m, 2H), 7.76 (d, 2H, ^3J *(H,H)* = 5,6Hz), 7.45 (d, 2H, ^3J *(H,H)* = 6 Hz), 7.26 (d, 2H, ^3J *(H,H)* = 5.2 Hz), 4.04 (m, 316H), 3.47 (dd, 4H, ^2J *(H,P)* = 22.8 Hz), 3.38 (dd, 4H, ^2J *(H,P)* = 22.4 Hz), 1.25-1.11 (m, 24H); ^{31}P-NMR ([D3]MeCN, 162 MHz): δ [ppm] = 22.82.; MS (MALDI): m/z = 832.65 $[(M-2PF_6)/2]^{2+}$, 1809.28 $[M-PF_6]^+$.; elemental analysis calcd. (%) for $C_{64}H_{72}Cl_2F_{12}N_{10}O_{12}P_6PtRu$: C = 39.34, H = 3.71, N = 7.17; found: C = 39.16, H = 3.85, N = 6.99.

$[Ru^{II}(tbbpy)_2bpyMeP](PF_6)_2$ (M)

A solution of **$[Ru^{II}(tbbpy)_2Cl_2]$** (0.125 g, 176 µmol) and bpyMeP (80.3 mg, 176 µmol) are refluxed in an ethanol/water mixture (30 mL/10 mL) for 20 h. During this time the color changed from deep brown to dark red. After removal of most of the ethanol at the rotary evaporator an excess of NH_4PF_6 was added to the solution The resulting red precipitate was collected, washed with water and diethyl ether and dried (78% yield).

^{1}H-NMR ([D3]MeCN, 400 MHz): δ [ppm] = 8.47 (s, 4H), 8.39 (s, 2H), 7.60-7.54 (m, 6H), 7.40-7.33 (m, 6H), 4.03 (m, 8H), 3.38 (d, 4H), 1.46-1.36 (m, 36H), 1.14 (t, 12H),; ^{31}P-NMR ([D3]MeCN, 162 MHz): δ [ppm] = 23.00

Crystals suitable for X-ray analysis were obtained by slow diffusion of Et_2O into a solution of the complex in acetone.
Crystal data: C62 H93 F12 N6 O7.50 P4 Ru, M_r = 1495.37 g mol^{-1}, red prism, crystal size 0.1211 x 0.0645 x 0.0487 mm^3, monoclinic, space group *C* 2/c, a = 46.4406(8) Å, b = 12.6539(2) Å, c = 30.2705(6) Å, β = 121.496(3)°, V = 15167.9(6) Å^3, T = 180(2) K, Z = 8, $\rho_{calcd.}$ = 1.310 Mg/m3, µ (Cu-Kα) = 3.162 mm^{-1}, F(000) = 6232, altogether 44485 reflexes up to h(-57/40), k(-15/15), l(-35/36) measured in the range of 7.517° ≤ Θ ≤ 73.818° , completeness Θ_{max} = 99.5 %, 14953 independent reflections, R_{int} = 0.0384, 11629 reflections with Fo > 4 σ(Fo), 864 parameters, 70 restraints, $R1_{obs}$ = 0.0555, $wR2_{obs}$ = 0.1549, $R1_{all}$ = 0.0705, $wR2_{all}$ = 0.1662, GOOF = 1.034, largest difference peak and hole: 1.145/-0.652 e·Å^{-3}. CCDC 1034963 contains the supplementary crystallographic data for this paper. These data can be obtained free of charge from The Cambridge Crystallographic Data Centre via www.ccdc.cam.ac.uk/data_request/cif. General remarks: Heavily disordered solvent molecules were removed from the experimental data using the Platon SQUEEZE routine. With respect to the calculated electron density, the solvent accessible void volume of 349.87 Å^3 (according to the Mercury Solvent Accessible Void calculation) supports the assumption that residual signals referred to a total of four molecules of diethylether per unit cell, i.e. 0.5 molecules of diethylether per formula unit. The cell contents were corrected accordingly in order to calculate appropriate crystal parameters.

General hydrolysis procedure

The ethylgroups of bpyMeP in $[Ru^{II}(tbbpy)_2bpyMeP](PF_6)_2$ **(3)** and **(4)** were removed as reported for $[Ru^{II}(bpy)_2(bpyMeP)]Cl_2$.[20]
The 1H-NMR-spectra of $[Ru^{II}(bpy(CH_2PO_3H_2)_2)_2(tpphz)]^{2+}$ and $[Ru^{II}(bpy(CH_2PO_3H_2)_2)_2(tpphz)PtCl_2]^{2+}$ were not interpretable as discussed above.

$[Ru^{II}(tbbpy)_2(bpy(CH_2PO_3H_2)_2)]^{2+}$

$[Ru^{II}(tbbpy)_2bpyMeP](PF_6)_2$ was hydrolyzed according to the general procedure.

^{1}H-NMR (([D3]MeCN, 400 MHz): δ [ppm] = 8.53 (s, 2H) , 8.46 (s, 4H), 7.82 (s, 2H), 7.53 (s, 2H), 7.42 (s, 4H), 7.36 (s, 2H), 7.21 (s, 2H), 2.95 (d, 4H), 1.40-1.28 (m, 36H); ^{31}P-NMR ([D3]MeCN, 162 MHz): δ [ppm] = 19.22.

Conclusions

$[Ru^{II}(bpyMeP)_2tpphzPtCl_2]^{2+}$ **(4)**, where bpyMeP is a bipyridine ligand substituted with ethyl phosphonic ester groups via a methylene spacer, was prepared and was utilized as a photocatalyst for hydrogen generation.
Resonance-Raman experiments revealed that the localization of the excited states in **(4)** are not changed fundamentally compared to $[Ru(tbbpy)_2tpphzPdCl_2]^{2+}$. Hence electron transfer in the direction of catalysis is guaranteed. In this process the methylene spacer between bpy and the anchoring moiety might play a role. The extent of the aromatic system of bpy is not altered by introducing *t*butyl- or $CH_2PO_3H_2$-groups.
Another important advantage of the methylene phosphonic ester groups, compared to carboxylic ester groups, is that there is no significant change of the photophysical properties compared to similar compounds without anchoring groups. This finding also might be attributed to the methylene spacer.
Deprotection of **(4)** goes along with solubility difficulties of the hydrolyzed product. One option to restore solubility in organic solvents might be treatment with a liphophilic cation like tbu_4N^+ as Graetzel *et al*. applied for the famous dye N719.[45] In this contribution **(4)** was successfully immobilized on NiO from aqueous NaOH solution (0.1 mM) and the sensitized film was analyzed by UV/Vis (reflection) spectroscopy.
Therefore a supramolecular building block approach towards photochemical molecular devices attached to electrode surfaces seems feasible.

Acknowledgements

This research was supported by the Studienstiftung des deutschen Volkes (MB), the German Research Association (DFG GRK 1626, MP), the Carl-Zeiss-Stiftung (DS), the CONCERT Japan and the COST Action CM1202, PERSPECT-H_2O.

Notes and references

[a] *M.Sc. Markus Braumüller, Dipl.-Chem. Michael Pfeffer, M.Sc. Dieter Sorsche, Dipl.-Chem. Markus Schaub, Prof. Dr. Sven Rau*
Universität Ulm, Anorganische Chemie I
Albert-Einstein-Allee 11, D-89081 Ulm, Germany
Fax: (+)49(0)731/50-23039
E-mail: Sven.Rau@uni-ulm.de

[b] *Dr. Martin Schulz, Prof. Dr. Benjamin Dietzek*
Institute of Photonic Technology (IPHT) Jena e. V,
Albert-Einstein-Straße 9, D-07745 Jena, Germany.
Tel: +49 3641206-332
E-mail: benjamin.dietzek@ipht-jena.de

[c] *Dr. Martin Schulz,Prof. Dr. Jürgen Popp, Prof. Dr. Benjamin Dietzek*
Institute for Physical Chemistry and Abbe Centre of Photonics
Friedrich-Schiller University Jena, Helmholtzweg 4, D-07743 Jena, Germany

[d] *Dr. Byung-Wook Park*
Department of Chemistry-Ångström, Uppsala University, Box 523, SE-751 20 Uppsala, Sweden,

[e] *Prof. Dr. Anders Hagfeldt*
Laboratory for Photomolecular Science (LSPM),
Swiss Federal Institute of Technology at Lausanne (EPFL), CH-1015 Lausanne, Switzerland.
E-mail: Anders.Hagfeldt@epfl.ch

[f] *Prof. Dr. Benjamin Dietzek*
Centre for Energy and Environmental Chemistry, Friedrich-Schiller-University Jena, Philosophenweg 7a, D-07743 Jena, Germany

† Electronic Supplementary Information (ESI) available:

DOI: 10.1039/b000000x/

1. E. S. Andreiadis, M. Chavarot-Kerlidou, M. Fontecave, and V. Artero, *Photochem. Photobiol.*, 2011, **87**, 946–64.

2. A. Hagfeldt, G. Boschloo, L. Sun, L. Kloo, and H. Pettersson, *Chem. Rev.*, 2010, **110**, 6595–663.

3. A. J. Esswein and D. G. Nocera, *Chem. Rev.*, 2007, **107**, 4022–4047.

4. Y. Pellegrin, L. Le Pleux, E. Blart, A. Renaud, B. Chavillon, N. Szuwarski, M. Boujtita, L. Cario, S. Jobic, D. Jacquemin, and F. Odobel, *J. Photochem. Photobiol. A Chem.*, 2011, **219**, 235–242.

5. M. Bräutigam, M. Schulz, J. Inglis, J. Popp, J. G. Vos, and B. Dietzek, *Phys. Chem. Chem. Phys.*, 2012, **14**, 15185–90.

6. Z. Ji, M. He, Z. Huang, U. Ozkan, and Y. Wu, *J. Am. Chem. Soc.*, 2013, **135**, 11696–9.

7. S. Rau, B. Schäfer, D. Gleich, E. Anders, M. Rudolph, M. Friedrich, H. Görls, W. Henry, and J. G. Vos, *Angew. Chem. Int. Ed. Engl.*, 2006, **45**, 6215–8.

8. M. Karnahl, C. Kuhnt, F. Ma, A. Yartsev, M. Schmitt, B. Dietzek, S. Rau, and J. Popp, *Chemphyschem*, 2011, **12**, 2101–9.

9. S. Tschierlei, M. Presselt, C. Kuhnt, A. Yartsev, T. Pascher, V. Sundström, M. Karnahl, M. Schwalbe, B. Schäfer, S. Rau, M. Schmitt, B. Dietzek, and J. Popp, *Chemistry*, 2009, **15**, 7678–88.

10. M. G. Pfeffer, L. Zedler, S. Kupfer, M. Paul, M. Schwalbe, K. Peuntinger, D. M. Guldi, J. Guthmuller, J. Popp, S. Gräfe, B. Dietzek, and S. Rau, *Dalton Trans.*, 2014, **43**, 11676–86.

11. M. G. Pfeffer, B. Schaefer, C. Kuhnt, M. Schmitt, J. Popp, L. G. G. Smolentsev, J. Uhlig, E. Nazarenko, V. Sundstroem, B. Dietzek and S. Rau, *Angew. Chem., accepted manuscript.* DOI: 10.1002/anie.201409438 and 10.1002/ange.201409438

12. W. Paw, W. B. Connick, and R. Eisenberg, *Inorg. Chem.*, 1998, **37**, 3919–3926.

13. B. Gholamkhass, K. Koike, N. Negishi, H. Hori, T. Sano, and K. Takeuchi, *Inorg. Chem.*, 2003, **42**, 2919–32.

14. R. B. Nair, B. M. Cullum, and C. J. Murphy, *Inorg. Chem.*, 1997, **36**, 962–965.

15. Y. Jenkins, a E. Friedman, N. J. Turro, and J. K. Barton, *Biochemistry*, 1992, **31**, 10809–16.

16. M. Schwalbe, M. Karnahl, S. Tschierlei, U. Uhlemann, M. Schmitt, B. Dietzek, J. Popp, R. Groake, J. G. Vos, and S. Rau, *Dalton Trans.*, 2010, **39**, 2768–71.

17. K. Hanson, M. K. Brennaman, A. Ito, H. Luo, W. Song, K. A. Parker, R. Ghosh, R. Lopez, and T. J. Meyer, *J. Phys. Chem. C*, 2012, **116**, 14837−14847.

18. L. Tong, A. Iwase, A. Nattestad, U. Bach, M. Weidelener, G. Götz, A. Mishra, P. Bäuerle, R. Amal, G. G. Wallace, and A. J. Mozer, *Energy Environ. Sci.*, 2012, **5**, 9472.

19. L. Li, L. Duan, F. Wen, C. Li, M. Wang, A. Hagfeldt, and L. Sun, *Chem. Commun. (Camb).*, 2012, **48**, 988–90.

20. I. Gillaizeau-Gauthier, F. Odobel, M. Alebbi, R. Argazzi, E. Costa, C. a Bignozzi, P. Qu, and G. J. Meyer, *Inorg. Chem.*, 2001, **40**, 6073–9.

21. T. Fujihara, M. Saito, A. Nagasawa, *Acta Crystallogr. Sect. E Struct. Reports Online*, 2004, E**60**, o262–o263.

22. G. Will, G. Boschloo, S. N. Rao, and D. Fitzmaurice, *J. Phys. Chem. B*, 1999, **1003**, 8067–8079.

23. S. Rau, B. Schäfer, A. Grüßing, S. Schebesta, K. Lamm, J. Vieth, H. Görls, D. Walther, M. Rudolph, U. W. Grummt, and E. Birkner, *Inorganica Chim. Acta*, 2004, **357**, 4496–4503.

24. T.-J. J. Kinnunen, M. Haukka, M. Nousiainen, A. Patrikka, and T. a. Pakkanen, *J. Chem. Soc. Dalt. Trans.*, 2001, 2649–2654.

25. D. Mulhern, S. Brooker, H. Görls, S. Rau, and J. G. Vos, *Dalton Trans.*, 2006, 51–7.

26. S. M. Zakeeruddin, K. Nazeeruddin, M. Gra, and C.- Lausanne, *Inorg. Chem.*, 1998, **37**, 5251–5259.

27. S. J. Smalley, M. R. Waterland, and S. G. Telfer, *Inorg. Chem.*, 2009, **48**, 13–15.

28. M. R. Norris, J. J. Concepcion, C. R. K. Glasson, Z. Fang, A. M. Lapides, D. L. Ashford, J. L. Templeton, and T. J. Meyer, *Inorg. Chem.*, 2013, **52**, 12492–501.

29. J. Bolger, A. Gourdon, and J. Launay, *J. Chem. Soc., Chem. Commun.*, 1995, **20**, 1799–1800.

30. D. Gut, A. Rudi, J. Kopilov, I. Goldberg, and M. Kol, *J. Am. Chem. Soc.*, 2002, **124**, 5449–56.

31. S. D. Bergman and M. Kol, *Inorg. Chem.*, 2005, **44**, 1647–54.

32. A. Juris, V. Balzani, F. Barigelletti, S. Campagna, P. Belser, and A. von Zelewsky, *Coord. Chem. Rev.*, 1988, **84**, 85–277.

33. L. Zedler, J. Guthmuller, I. Rabelo de Moraes, S. Kupfer, S. Krieck, M. Schmitt, J. Popp, S. Rau, and B. Dietzek, *Chem. Commun.*, 2014, **50**, 5227--5229.

34. Y. Liu, A. Chouai, N. N. Degtyareva, D. a Lutterman, K. R. Dunbar, and C. Turro, *J. Am. Chem. Soc.*, 2005, **127**, 10796–7.

35. D. a Lutterman, A. Chouai, Y. Liu, Y. Sun, C. D. Stewart, K. R. Dunbar, and C. Turro, *J. Am. Chem. Soc.*, 2008, **130**, 1163–70.

36. J. Bolger and J. Launay, *Inorg. Chem.*, 1996, **35**, 2937–2944.

37. S. Tschierlei, M. Karnahl, M. Presselt, B. Dietzek, J. Guthmuller, L. González, M. Schmitt, S. Rau, and J. Popp, *Angew. Chem. Int. Ed. Engl.*, 2010, **49**, 3981–4.

38. M. Wächtler, J. Guthmuller, L. González, and B. Dietzek, *Coord. Chem. Rev.*, 2012, **256**, 1479–1508.

39. M. Karnahl, C. Kuhnt, F. W. Heinemann, M. Schmitt, S. Rau, J. Popp, and B. Dietzek, *Chem. Phys.*, 2012, **393**, 65–73.

40. C. Pehlken, R. Staehle, D. Sorsche, C. Streb, and S. Rau, *Dalton Trans.*, 2014, **43**, 13307–13315.

41. S. Pailloux, C. E. Shirima, K. A. Smith, E. N. Duesler, R. T. Paine, N. J. Williams, and R. D. Hancock, *Inorg. Chem.*, 2010, **49**, 9369–79.

42. G. M. Sheldrick, *Acta Crystallogr. A.*, 2008, **64**, 112–22.

43. N. Vriamont, B. Govaerts, P. Grenouillet, C. de Bellefon, and O. Riant, *Chemistry*, 2009, **15**, 6267–78.

44. A. R. Oki and R. J. Morgan, *Synth. Commun.*, 1995, **25**, 4093–4097.

45. K. Nazeeruddin, S. M. Zakeeruddin, M. Jirousek, P. Liska, N. Vlachopoulos, V. Shklover, C. Fischer, M. Gra, C.- Lausanne, and R. V August, *Inorg. Chem.*, 1999, **38**, 6298–6305.

